Mechanism of Collapse of Tall Steel Moment Frame Buildings Under Earthquake Excitation

S. Krishnan & M. Muto
California Institute of Technology

SUMMARY:
We expound on the nature of collapse of one class of tall buildings (steel moment frame buildings) under earthquake excitation. Using a parametric analysis of a couple of index buildings subjected to idealized ground motion histories, we establish the ground motion features that cause collapse in these structures. Systematically mapping damage localization patterns, we track the evolution of the collapse mechanism. We demonstrate the existence of a select few preferred mechanisms of collapse in these buildings and describe the associated physics using wave propagation through a shear beam. A simple theory based on work-energy principles can identify these mechanisms.

Keywords: Collapse mechanism, tall steel moment frame buildings, earthquakes, plasticity, fracture

1. INTRODUCTION

Ever since the collapse of two tall steel buildings in the 1985 Mexico City earthquake, there has been sustained interest in understanding the response of tall steel buildings under strong earthquake excitation through simulations. Steel building damage observations during the 1994 Northridge and the 1995 Kobe earthquakes further led to several studies investigating the causes of this damage [e.g., SAC (1995), Challa and Hall (1995)]. All these studies provide insights into the nature of tall steel moment frame building to earthquake excitation. But they are not comprehensive and systematic in exploring the evolution of damage and the formation of the mechanism of collapse. Questions such as "where does damage localize over the building height?", "does this depend on the frequency content and amplitude of ground shaking?", "can a relationship be developed between these features of the ground motion and the region of damage localization?", "could there be more than one damage localization region?", "if so, when and which of these regions evolves into a collapse mechanism?", "are there any preferred mechanisms of collapse in these buildings?", "if so, can these be determined independent of the ground motion?", have not been answered in a comprehensive and conclusive manner. Here, we make an attempt to address these questions through computational case-history studies of two 18-story steel moment frame buildings and their variants.

The first building is an existing 18-story office building, located within five miles of the epicenter of the 1994 Northridge earthquake. An isometric view of its FRAME3D model is shown in Figure 1a. It was designed according to the 1982 Uniform Building Code (UBC) and completed in 1986-87. The height of the building above ground is 75.7 m (248' 4") with a typical story height of 3.96 m (13' 0") and taller first, seventeenth, and penthouse stories. The lateral force-resisting system consists of two-bay welded steel moment-frames, two apiece in either principal direction of the structure (Figure 1b). The location of the north frame one bay inside of the perimeter gives rise to some torsional eccentricity. Many moment-frame beam-column connections in the building fractured during the Northridge earthquake, and the building has been extensively investigated since then by engineering research groups [e.g., SAC (1995)]. Fundamental periods, computed assuming 100% dead load and 30% live load contribution to the mass, are 4.52s (X-translation), 4.26s (Y-translation) and 2.69s (torsion). We consider two models of the existing building, one with connections susceptible to fracture, and the other with perfect connections. Two orthogonal orientations (with respect to the strong component of the ground motion) are considered for the model with perfect connections.

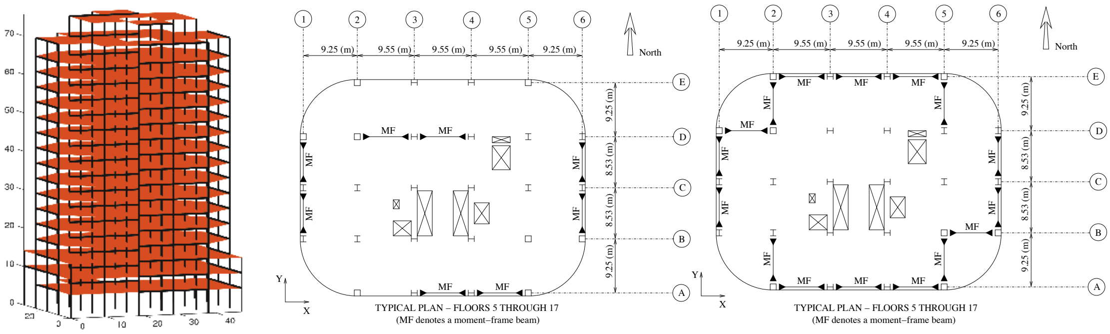

Figure 1. (a) Existing building (1982 UBC design) FRAME3D model; (b) Existing building typical floor plan; (c) Redesigned building (1997 UBC design) typical floor plan.

The second building is similar to the existing building, but the lateral force-resisting system has been redesigned according to the 1997 UBC. It has been designed for larger earthquake forces and greater redundancy in the lateral force-resisting system, with 8 bays of moment-frames in either direction [although lateral resistance will likely be dominated by the three-bay moment frames (Figure 1c) as opposed to the single-bay moment frames]. The frame located in the interior of the existing building has been relocated to the exterior, eliminating the torsional eccentricity. Of course, torsion may still occur in the building as a result of differential yielding in the moment frames. Fundamental periods, computed assuming 100% dead load and 30% live load contribution to the mass, are 4.06s ([X+Y-] translation), 3.85s ([X+Y+] translation) and 2.60s (torsion). Note that the fundamental translational modes are oriented approximately along diagonals on the building plan view. Only one variant of the redesigned building is modeled here, that with perfect connections.

2. GROUND MOTION IDEALIZATION SCHEME

The sensitivity of tall building response to peak ground velocity can be established using the classical, but approximate, analysis of energy budget in multi-story buildings subjected to earthquake excitation [e.g., Uang and Bertero (1990)]. It can be shown that for the long-period buildings of this study, while the energy imparted from short-period excitation is small and the peak transient interstory drift ratio (IDR) must consequently be quite small, the energy imparted by excitation with period much longer than that of the structure is proportional to the square of the ground velocity. In other words, for the long-period structures of this study, only long-period ground motion can induce a strong response; and this response is extremely sensitive to the peak ground velocity (PGV). These observations suggest that the best candidate for idealization in as far as ground motion time histories is concerned is the ground velocity history. The three most important parameters in the idealization scheme must be the frequency content of the time history (period of predominant shaking), the peak ground velocity, and the duration represented by the number of cycles. Here, ground velocity time histories are idealized as triangular (sawtooth-like) wave-trains (Figure 2). The displacement history in this representation closely mimics the displacement pulse that would result from the rupture of a penny-shaped crack on a fault surface (point-source) in the vicinity of the crack. Although a single cycle is shown in the figure, multi-cycle extensions with identical period and amplitude are also used to represent long-duration ground motion time histories. The acceleration time history corresponding to this velocity history is a rectangular wave-train, while the displacement is a one-sided parabolic wave-train. Three parameters are used to characterize the ground velocity time history: period T, amplitude PGV (peak ground velocity), and number of cycles N. The ability of this ground motion representation to accurately emulate the true seismic ground motion time histories in as far as impacts on the buildings of interest are concerned must be ensured. Toward this end, the best-fitting single-cycle idealized time history from a suite of idealized time histories to the strong component of 18 near-source records (velocity histories) is determined using the Least Absolute Deviation method (L_1 norm). The idealized time history suite comprises of time histories with period varying between 0.5s and 6.0s at 0.25s intervals, PGV varying between 0.125m/s and 2.5m/s at 0.125m/s intervals, and the number of cycles N taking the values of 1 to 5 as well as 10 to emulate long duration records. The near-source records are from the 1971 San Fernando, the 1978 Iran, the 1979 Imperial Valley, the 1987 Superstition Hills, the 1989 Loma Prieta, the 1992 Cape Mendocino, the 1992 Landers, the 1994 Northridge, the 1995 Kobe, and the 1999 Chi-Chi earthquakes. The FRAME3D models of the existing building (perfect and susceptible connections), and the redesigned building (perfect connections) are analyzed under the 18 three-component near-source records. For the existing building model with susceptible connections and the redesigned building model with perfect connections, the strong component of ground motion is oriented in the building X direction. For the existing building model with perfect connections, two cases are considered: strong component oriented in the building X and Y directions. The same models are also analyzed under the one-component best-fitting single-cycle idealized time histories. Shown in Figure 3 is the comparison of the profiles of peak transient IDR over the height under the actual and idealized motions for the existing building (susceptible connections) model for two ground motion cases. The good match of the profiles indicates that the particular idealization adopted here to characterize the ground motion can be very effectively used in studying the response of the target buildings. The peak values of IDR in all four building models from the two sets of analysis are compared against each other and the errors are also quantified in the figure. The mean and standard deviation of the best-fitting Gaussian distribution function to the IDR errors are 0.00056 and 0.0069, respectively. All 18 ground motion cases are included in this calculation.

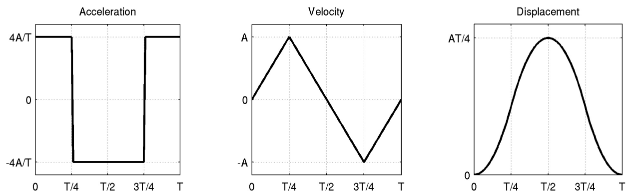

Figure 2. Acceleration, velocity, and displacement histories of idealized pulses used as input ground motions.

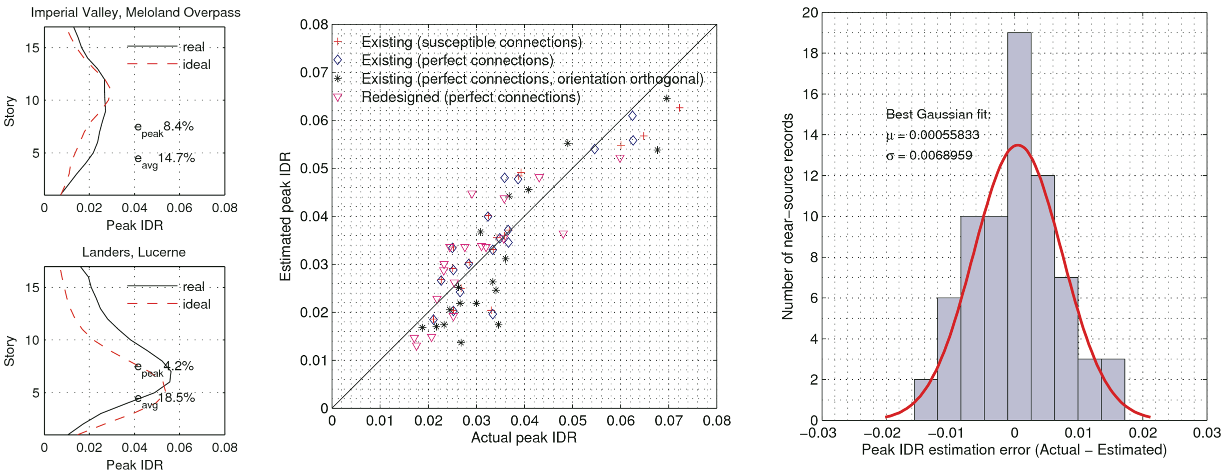

Figure 3. Comparison of peak transient interstory drift ratio (IDR) profile over building height computed using real record against that computed using the best-fit idealized 1-cycle saw-tooth time history: Existing building (susceptible connections). Also shown are peak transient interstory drift ratio (IDR) in all the building models computed using the near-source records plotted against that estimated using best-fit idealized 1-cycle saw-tooth time histories along with the histogram of and the best-fitting Gaussian distribution to the estimation error.

3. STRUCTURAL RESPONSE TO IDEALIZED GROUND MOTION

To explore the nature of damage localization and the evolution of the collapse mechanism as a function of ground motion features, a series of 3-D nonlinear response history analyses are conducted on the four building models: (a) Existing building (susceptible connections) under X direction excitation, (b) Existing building (perfect connections) under X direction excitation, (c) Existing building (perfect connections) under Y direction excitation, and (d) Redesigned building (perfect connections) under X direction excitation. The models are subjected to the idealized 1-component ground motion time histories introduced in the last section with ground motion period T varying between 0.5s and 6.0s at 0.25s intervals, PGV varying between 0.125 m/s and 2.5 m/s at 0.125 m/s intervals, and the number of cycles N taking the values of 1 to 5 and 10. Key response metrics are computed and stored in a database. These include the peak transient IDR and its location over the building height, the peak residual IDR and its location, permanent roof drift (or tilt) following seismic shaking, plastic rotations in beams, columns, and joints (panel zones), and locations of fractures in the model with fracture-susceptible connections. For the peak transient IDR, the larger of the peak values at two diagonally opposite corners of each story is taken in order to accurately include the effects of torsion in the performance assessment. The peak residual IDR is computed by lowpass-filtering the interstory drift ratio histories and averaging the points within a 5s time-window that has the lowest variance of all such time-windows in the record. A two-pass Butterworth filter with a corner at 10s is employed. A similar approach is adopted for computing the permanent roof drift which is the roof residual displacement normalized by building height. The results for each building model, in the form of maps and/or figures, are catalogued in a comprehensive report [Krishnan and Muto (2011)].

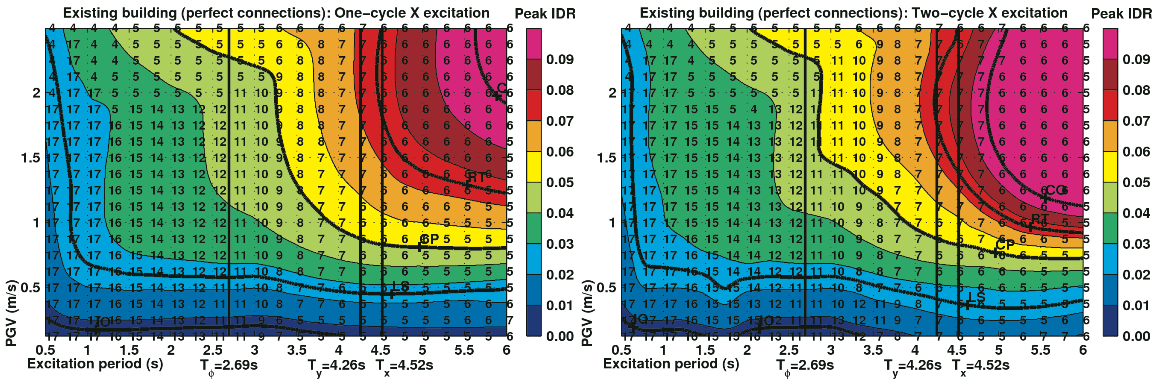

Figure 4. Peak transient IDR maps on the T−PGV plane for the existing building (perfect connections) under 1- and 2-cycle idealized X-direction ground motion. The story location where the peak occurs is labeled at each of the 460 [T,PGV] combinations for which analyses were performed. Contours corresponding to the empirical immediate occupancy (IO), life-safety (LS), collapse prevention (CP), red-tagged (RT), and collapsed (CO) performance levels are shown. The principal direction building fundamental periods are indicated for reference.

Shown in Figure 4 are maps of peak transient IDR on the PGV−T plane for the existing building model with perfect connections under idealized 1- and 2-cycle excitation applied in the X direction. The data from the parametric analysis computed at discrete values of T and PGV is first interpolated on a fine parameter grid using a triangle-based linear interpolation technique. It is then filtered using a disk-shaped correlation filter to smoothen sharp transitions in the contours. Also plotted on the maps are contours corresponding to the upper limits on IDR of the Federal Emergency Management Agency (FEMA [9]) performance levels of Immediate Occupancy (IO; IDR=0.007), Life Safety (LS; IDR=0.025), and Collapse Prevention (CP; IDR=0.05). Contours corresponding to peak transient IDRs of 0.075 (Red-Tagged, RT) and 0.100 (Collapsed, CO) are shown as well. Gravity-driven progressive collapse invariably takes hold of our numerical models beyond peak transient IDRs of 0.100. However, since our models do not include degradation due to local flange buckling, we believe the probability of collapse in real-world buildings to be significant beyond peak transient IDR values of 0.075. That said, for the purposes of this paper, definitive inferences on collapse can be made from the analyses of this study only at peak transient IDR of 0.100. Figure 4 shows that for collapse to occur in the model with perfect connections under 1- or 2-cycle excitation (e.g., near-source records), the excitation period must exceed roughly the building fundamental period of 4.5s. This is in agreement with the theoretical energy balance analysis alluded to earlier. Collapse-level response is induced only by long-period ground motions. Under such motions, the structural response degrades rapidly as a result of a quadratic growth in input energy with increasing PGV. If the intensity of shaking (PGV) is very strong, then the period does not have to be as long to induce collapse-level response. Alternately, within certain limits, a longer period motion relative to the building fundamental period requires a smaller PGV to cause collapse-level response. These findings apply to the PGV range of 0-2.5m/s and an excitation period range of 0-6s. If ground motion period is much longer (greater than, say, twice or thrice the fundamental period of the building), then loading is almost static and does not induce strong enough dynamic response. The story location of peak transient IDR closely tracks the ground excitation period T, steadily dropping from the top of the building with increasing T. The downward migration halts not at the bottom story, but slightly higher.

4. QUASI-SHEAR BAND AND CHARACTERISTIC MECHANISM FORMATION

To first illustrate the anatomy of a collapse mechanism, one typical instance of simulated collapse is dissected and presented here. The existing building model collapses when subjected to synthetic 3-component motion at Northridge from an 1857-like magnitude 7.9 earthquake on the San Andreas fault. The deformed shape of the structure as it is collapsing, along with the plastic hinges on one of the frames, is shown in Figure 5. The figure shows the formation of plastic hinges at the top of all columns in an upper story, at the bottom of all columns in a lower story, and at both ends of all beams in the intermediate stories. Such a pattern of hinging results in shear-like deformation in these stories, resembling plastic shear bands in ductile solids that are severely (shear) strained [e.g., Rice (1976)]. We coin the term "quasi-shear band (QSB)" to refer to this yield localization region in moment frame buildings. Most of the lateral deformation due to seismic shaking is concentrated in this band. The severe plastic hinging causes it to be far more compliant than the overriding block of stories above and the supporting basal block of stories below. When the overturning 1st-order and 2nd-order (P$-\Delta$) moments from the inertia of the overriding block of stories exceeds the moment-carrying capacity of the fully plasticized quasi-shear band (and if the subsequent seismic waves impart a velocity to the base that is opposite in direction to that of the block of stories over-riding the QSB), it loses stability and collapses. This initiates gravity-driven progressive collapse of the overriding block of stories. Thus, the collapse mechanism initiates as a sidesway mechanism that is taken over by gravity once the quasi-shear band is destabilized. This mode of collapse was predicted by Lignos et al. (2011) through analysis and subsequently realized in earthquake simulator tests of two 1:8 scale models of a 4-story code-compliant steel moment frame building. A similar sidesway collapse mode was observed in a full-scale 4-story steel moment frame building that was shaken by the Takatori record from the 1995 Kobe earthquake on the E-Defense Shake Table in Japan [Suita et al. (2008)].

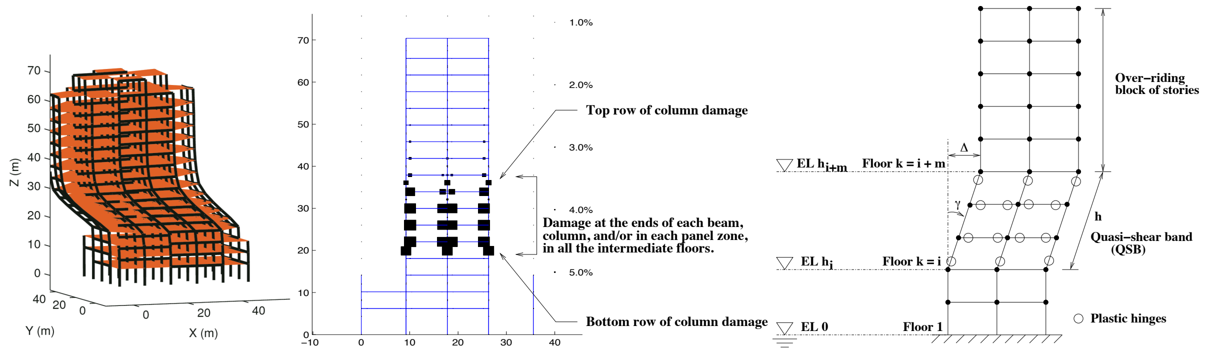

Figure 5. Anatomy of a collapse mechanism: (a) Typical mechanism of collapse from the simulation of the existing building subjected to strong ground motion (synthetic 3-component motion at Northridge from an 1857-like Mw = 7.9 earthquake on the San Andreas fault). Deformations are scaled by a factor of 5 for visual clarity. (b) Plastic rotations at the ends of beams and columns (squares) in one of the frames oriented in the direction of sidesway collapse. (c) Simplified schematic of a sidesway-collapse mechanism.

An idealized representation of the collapse mechanism is shown in Figure 5c. In structures where the moment frame is proportioned such that the panel zones are weaker than the beams, the quasi-shear band may start with yielding in the panel zones of the intermediate stories rather than at the ends of the beams. However, shear yielding of panel zones is quite a stable mode of deformation (note that the material model for panel shear stress-strain behavior in FRAME3D has no upper limit on the shear strain). Well before some form of instability sets in the panel zone region, there will typically be sufficient moment build-up in the beams to cause yielding. Since deterioration can be much faster in beams, the eventual collapse mechanism will be due to excessive plastic rotations in the beams of the intermediate stories of the quasi-shear band. In an N_s-story building, N_s 1-story quasi-shear bands are theoretically possible, (N_s-1) 2-story QSBs are possible, and so on [Krishnan and Muto (2012)]. Thus, there are a total of $N_s(N_s+1)/2$ possible QSBs in either principal direction of the building. During strong shaking one or more of these quasi-shear bands can form. It is reasonable to postulate that the most prominent of these bands, the "primary" quasi-shear band, will evolve into a sidesway collapse mechanism. Then, in order to help establish the relationship between the collapse mechanism of the buildings considered in this study and the ground motion parameters, T, PGV, and N, the first step would be to identify the primary quasi-shear band in each of the analysis cases archived in the database of Section 3. This is accomplished by attributing and computing a damage index for each of the $N_s(N_s+1)/2$ possible quasi-shear bands. The band with the largest damage index is the "primary" quasi-shear band. This damage index is an aggregate of the damage indices (extent of plasticity) of all the components comprising the band [Krishnan and Muto (2012)].

Shown in Figure 6a is the variation of the three floor damage indices (average of column top damage, average of column bottom damage, and average of joint damage) over the height of the existing building (perfect connections) when subjected to strong 3-component ground motion simulated at a southern California site in the ShakeOut scenario earthquake [Muto and Krishnan (2011)]. Also shown is the identified primary quasi-shear band (red dashed line). It is clear from the actual distribution of frame plastic hinging (Figure 6b) that there is uniformly heavy yielding throughout the identified primary QSB. While there is some beam yielding above and below this band, collapse is not likely to extend beyond the stories within the selected band because significant column yielding has occurred only at the upper and lower limits of this band and not outside. This can be seen from Figure 6a which shows that the top and bottom of the primary QSB correspond to local maxima of the floor damage indices computed using the column top and bottom damage, respectively.

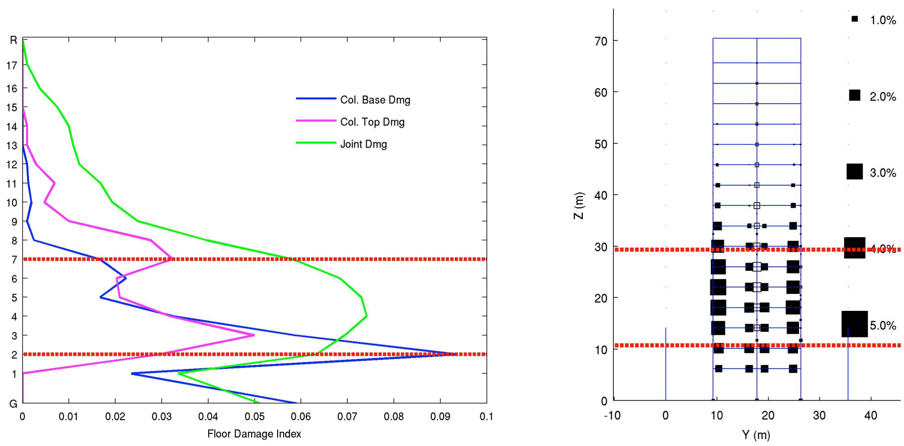

Figure 6. (a) Identification of the primary quasi-shear band (QSB). (b) Comparison of the identified primary QSB against the actual distribution of plastic hinges in the existing building (perfect connections) when subjected to strong 3-component ground motion simulated at a southern California site in the ShakeOut scenario earthquake.

The identified QSBs in the existing building (perfect connections) under the idealized 1-cycle X-direction ground excitation are shown in Figure 7. Shown there are bars indicating the location and extent of the primary quasi-shear band over the height of the building as a function of the excitation period T, for each PGV intensity. The fill color represents the peak transient IDR. There is no column damage when the pulse amplitude is less than or equal to 0.5 m/s for any pulse period in the range 0.5-6.0s. Hence, no quasi-shear band has formed and none could be identified in these cases. For a given pulse in the relatively low amplitude regime (0.125-1.375 m/s), say with amplitude 1.25 m/s, the primary QSB is located at the top of the building for small pulse period and migrates down with increasing pulse period. This downward migration stops at the third or fourth floor for pulse periods longer than about the fundamental period of the building, with the location of the band becoming invariant with ground excitation period. For a given pulse in the relatively large amplitude regime (1.875-2.5 m/s), say with amplitude 2.00 m/s, the primary quasi-shear band is located at the bottom of the building for small pulse period and migrates up with increasing pulse period until it coalesces nominally to the same invariant QSB location as for pulses in the low-amplitude, long-period excitation regime discussed above. For a pulse in the intermediate amplitude regime (1.50-1.75 m/s), say with amplitude 1.50 m/s, the primary QSB is located at the bottom stories for short periods, at the top stories for intermediate periods (< building fundamental period) and migrating down with increasing period. The migration once again stops (when the pulse period roughly equals the fundamental period of the building) nominally at the same invariant QSB location as was observed for the low-amplitude and large-amplitude, long period excitation regimes. These observations more or less hold true for all four building models (existing building with susceptible connections under X excitation, existing building with perfect connections under X and Y excitation, and redesigned building with perfect connections under X excitation) subjected to 1-cycle excitation [Krishnan and Muto (2011)]. There are subtle differences from one case to the next. However, under long period excitation in both the low amplitude and high amplitude regimes, the convergence of the primary quasi-shear band to one or two building-specific sets of stories holds true in majority of the cases.

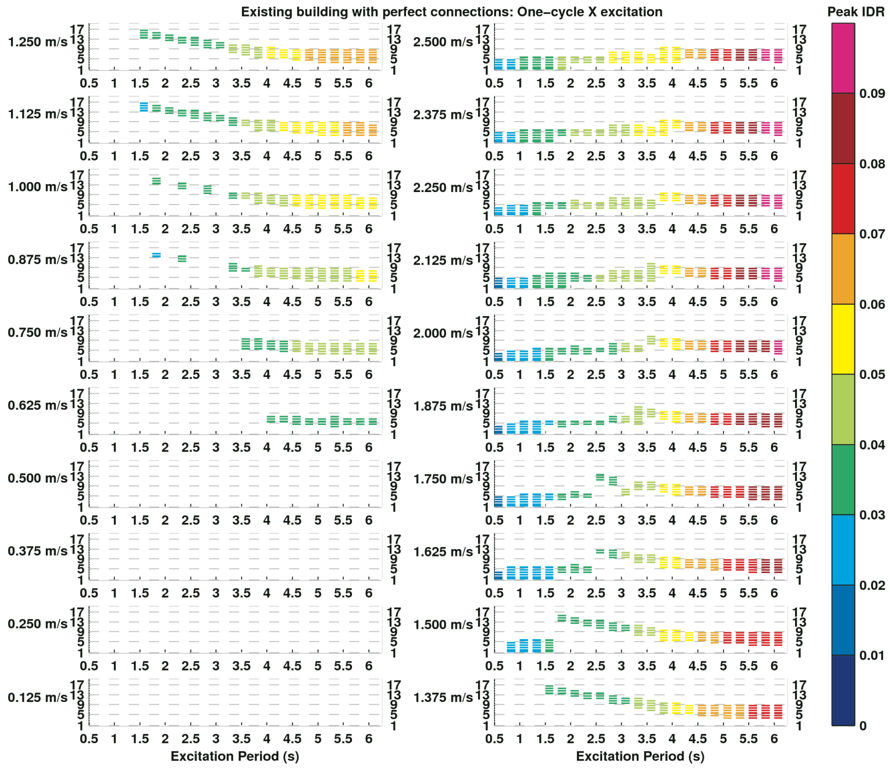

Figure 7. Primary quasi-shear band (QSB) in the existing building (perfect connections) subjected to idealized single- cycle X direction excitation. Pulse period T varies from 0.5 seconds to 6 seconds; peak ground velocity P GV varies from 0.125 m/s to 2.5 m/s.

The results for multi-cycle excitation are quite similar to those under single-cycle excitation, except that the PGV thresholds demarcating low-, moderate-, and high-intensity ground motions are progressively lower with increasing number of cycles. The excitation period thresholds for collapse are lower as well. But, collapse continues to occur nominally in the same set of stories under multi-cycle excitation as for the single-cycle excitation. It should be pointed out, however, that degradation due to local flange buckling, which is not included in the analysis, may have a bigger influence under multi-cycle excitation, rendering the analysis results less accurate. Figure 8 shows the primary quasi-shear band in the existing building (susceptible connections) and the redesigned building model (perfect connections) under 1- and 3-cycle X excitation, re-arranged in the order of increasing peak interstory drift ratio (IDR). It is clear that with few exceptions collapse (peak transient IDR > 0.100) occurs only in cases where the primary quasi-shear band has formed in the set of stories corresponding to the nominally invariant QSB that forms under 1-cycle excitation. This suggests a characteristic mechanism or one or two preferred mechanisms of collapse for each building under all forms of earthquake excitation. For instance, there is a strong preference for collapse to occur between floors 3 and 9, floors 3 and 10, and floors 4 and 10 in the existing building (susceptible connections) under X direction excitation. There is a weaker preference for collapse to occur between floors 5 and 10, and 5 and 11. Thus, there are just five preferred mechanisms out of a total of 153 possible mechanisms. Similarly, there is a strong preference for collapse to occur between floors 3 and 8 in the redesigned building (perfect connections) under X excitation. There is a weak preference for collapse to occur between floors 4 and 9, floors 3 and 9, floors 3 and 6, and floors 3 and 7 (five preferred mechanisms out of [$N_s(N_s+1)/2$ = 153] possible mechanisms). Note that the preferred collapse mechanisms are spatially clustered together with significant story-overlap. Collapse is restricted to occur in this narrow band of stories. Similar results are observed for the existing building model with perfect connections under X direction and Y direction excitations [Krishnan and Muto (2011)]. The occurrence of just 1–5 preferred collapse mechanisms that are clustered together in the simulations of all four models can be explained through the shear beam analogy [Krishnan and Muto (2012)].

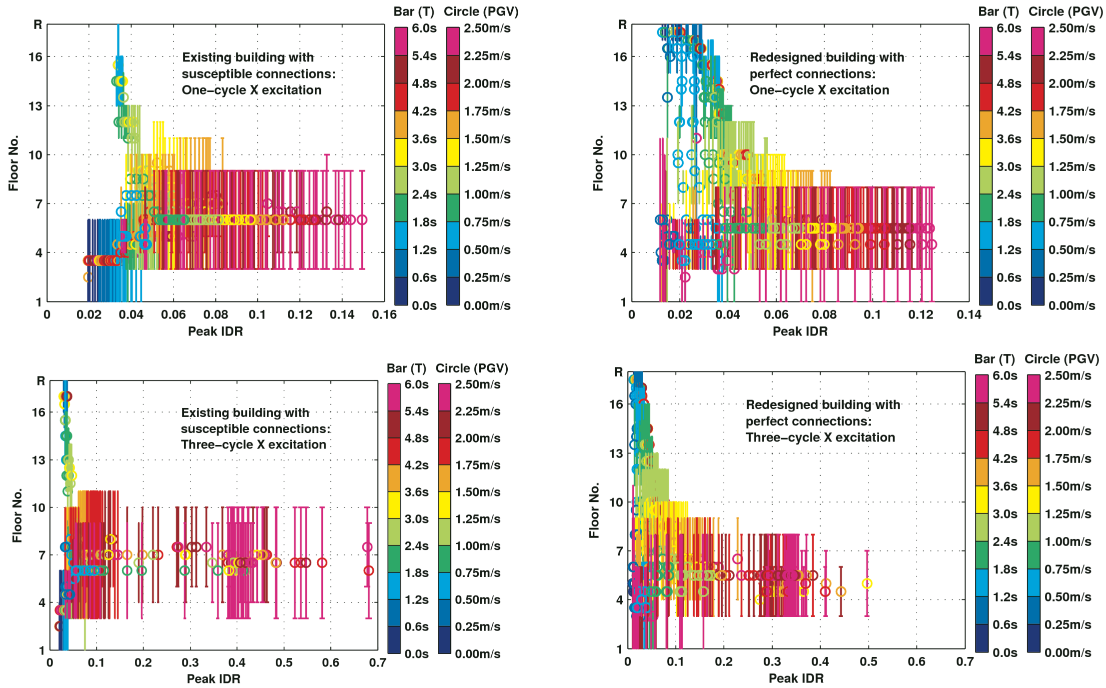

Figure 8. The location and extent of the primary quasi-shear band (QSB) plotted against peak interstory drift ratio (IDR) in the existing building (susceptible connections) and the redesigned building (perfect connections) models when subjected to idealized 1- and 3-cycle X direction excitation. Ground excitation T and PGV can be identified by pen color of bar and circle, respectively.

The distribution of moments in a steel moment frame subjected to lateral loads is such that it produces double curvature in all the columns and beams resulting in shear-racking of the frame. Thus, in an overall sense, shear-beam-like behavior and not cantilever-like behavior dominates moment-frame response. This allows for the drawing of an analogy between steel moment frames excited by earthquake ground motion and a shear wave traveling through a uniform shear-beam. However, three significant differences exist between steel moment frame buildings and uniform shear-beams. First, the buildings are not uniform, there is typically stiffness and strength gradation as well as some mass variation over the height of the structure. Second, gravity is not usually considered in the uniform shear-beam, whereas it plays an important role in the collapse behavior of the building structure by causing second order (P−Δ) effects associated with the self-weight of the structure acting through its deformed configuration under lateral loading. P−Δ effects, however, simply amplify the 1st order overturning moments caused by the floor plate inertial forces. This amplification becomes perceptible only beyond peak transient IDRs of 0.025 and becomes significant beyond peak transient IDRs of 0.05 [Krishnan and Muto (2011, 2012)]. At the peak transient IDR level of 0.05, the primary quasi-shear band has typically coalesced and become invariant (e.g., Figures 7 and 8), suggesting that P−Δ effect has only a minor role to play in the formation of the quasi-shear band. Lastly, steel-frame buildings do exhibit low levels of damping which are not typically present in the uniform shear-beam. Damping has the effect of attenuating the response (which impacts the response to multi-pulse excitation more than single-pulse excitation) and lengthening the apparent period. But the low level of damping inherent in steel structures means that it plays a relatively minor role in the damage localization phenomenon. Thus, the differences in the building response and the analogous shear-beam response, if they exist, are attributable primarily to non-uniformity.

Under low-intensity motions (PGV < 0.25m/s) with periods in the 0.5s-6s range excitation energy is low. As a result, structural response is predominantly elastic and is analogous to that of a uniform elastic shear-beam through which a shear wave propagates. For moderate-intensity excitations (0.25m/s ≤ PGV < 1.5m/s), the reverse phase of the incident pulse constructively interferes with the reflected forward phase causing yielding in the region of positive interference, very similar to what would occur in a uniform inelastic shear-beam. The primary quasi-shear band migrates down the building with increasing pulse period. However, this migration slows down with increasing period and gets arrested nominally between floors 3 and 9 for the existing building, and between floors 3 and 8 for the redesigned building, whereas the peak strain in the corresponding inelastic uniform shear-beam continues to migrate to the very bottom. This is a direct result of the non-uniformity of the buildings. Going from the top of the building to the bottom, there is a gradual increase in the strength and stiffness of the structure. The increased strength at the bottom does not allow yielding to permeate into those stories. Now, excitation energy can be large enough only under long-period ground motion in the context of the target buildings (from the classical energy budget analysis). Therefore, collapse-level response must be accompanied by the formation of the primary quasi-shear band in the vicinity of the stories where the downward migration of the QSB (with increasing T) is arrested.

For high-intensity excitations (PGV > 1.5m/s) that are sufficiently long-period, the pulse may yield the structure on its way up the building. The strength of the building drops as the pulse travels up the building. However, inertial forces drop as well, as a result of fewer stories above contributing to the mass. The narrow band of stories with an optimal combination of low-enough strength and high-enough inertial force demand is where peak yielding occurs. This region is identical to the region where the downward migration of the primary quasi-shear band is arrested under moderate-intensity, long-period excitation. This is because the governing factor dictating the location of the band in both cases is strength non-uniformity. As the wave travels up the building, it is reflected off the roof with a change in sign. Because the period of the incident wave is sufficiently long (a necessary condition for large input excitation energy from the energy budget analysis), the reverse phase of the incident pulse constructively interferes with the reflected forward phase causing greatest yielding in the same region as the pre-reflection yielding. To summarize, under both moderate-intensity and high-intensity ground motions, input excitation energy large enough to collapse the building requires long-period excitation. Such long-period excitation always causes the formation of the primary quasi-shear band in an optimal set of stories governed by the mass and strength distribution of the building over its height, which are characteristics solely of the structure and not the ground motion. When T and PGV are large enough, it is this band that evolves into a collapse mechanism.

5. IDENTIFYING THE CHARACTERISTIC COLLAPSE MECHANISM

The principle of virtual work can be applied to each of the $N_s(N_s+1)/2$ possible quasi-shear bands in either principal direction of the building, at the instant that the QSB has been fully plasticized. This analysis would result in an expression for the critical acceleration of the overriding block that would cause the QSB to fully plasticize for each band [Krishnan and Muto (2011, 2012)]. From plastic analysis principles, the quasi-shear band that becomes unstable (completely plasticizes) at the lowest acceleration of the over-riding block is the characteristic plastic mechanism of collapse. The characteristic mechanisms of collapse for all cases are well identified using this approach. For example, the collapse mechanism predicted for the existing building X direction extends from floor 3 to floor 10 at a critical acceleration of 0.130g. The critical accelerations for QSBs that run from floors 3 to 9 and 3 to 8 are not too different (0.131g and 0.132g), these QSBs could evolve into collapse mechanisms as well. Thus, three preferred mechanisms may be predicted using this approach and these are the strongly preferred mechanisms observed in the simulations (Figure 8).

6. CONCLUSIONS

Based on case studies of two tall steel moment frame buildings subjected to idealized 1-component ground motion time histories (11040 simulations) as well as synthetic 3-component seismic time histories (1908 simulations), we predicate the existence of a characteristic mechanism of collapse or a few preferred mechanisms of collapse. The evidence presented is most credible for 1- or 2-cycle near-source excitation since the numerical models do not include local flange buckling which would become more important under multi-cycle excitation. Damage (yielding and/or fracture) localizes in a few stories to form a "quasi-shear" band. When the band is destabilized, sidesway collapse is initiated and gravity takes over. Using classical energy balance analysis and the shear beam analogy it has been shown that under collapse-inducing long-period, moderate- to large- amplitude motions, the critical quasi-shear band in the typically non-uniform buildings must occur in an optimal set of stories where the strength of the structural elements is low enough, but the driving mass of the over-riding floors is sufficiently large. The location of this critical band does not depend upon the finer details of the ground motion. A convenient plastic analysis approach has been developed to ascertain the potential of each of the possible quasi-shear bands in a building to collapse. The characteristic and/or preferred collapse mechanisms identified by this method agree well with the simulations of all the tall building models. The method can alternately be used to develop an improved design of the building that would be close to optimal, where yielding occurs all over, by proportioning the system to make all collapse mechanisms equally likely.

ACKNOWLEDGEMENT
This study was funded in part by the U.S. National Earthquake Hazard Reduction Program (NEHRP award number G09AP00063).

REFERENCES

SAC (1995). Analytical and Field Investigations of Buildings Affected by the Northridge Earthquake of January 17, 1994. Tech. Rep. 95-04, Parts 1 and 2, SEAOC, CUREE, ATC, USA.

Challa, V.R.M. and Hall, J.F. (1994). Earthquake Collapse Analysis of Steel Frames. *Earthquake Engineering and Structural Dynamics* **23:11**, 1199-1218.

Uang, C.-M. and Bertero, V.V. (1990). Evaluation of Seismic Energy in Structures. *Earthquake Engineering and Structural Dynamics* **19:1**, 77-90.

Krishnan, S. and Muto, M. (2011). Mechanism of Collapse, Sensitivity to Ground Motion Features, and Rapid Estimation of the Response of Tall Steel Moment Frame Buildings to Earthquake Excitation. Tech. Rep. EERL 2011-02, Earthquake Engineering Research Laboratory, California Institute of Technology, Pasadena, California, USA.

Rice, J.R. (1976). The Localization of Plastic Deformation. *14th International Congress on Theoretical and Applied Mechanics*, W. T. Koiter, Ed., North-Holland Publishing Co., Delft, **Vol I:** 207–220.

Lignos, D.G., Krawinkler, H., and Whittaker, A.S. (2011). Prediction and Validation of Sidesway Collapse of Two Scaled Models of a 4-Story Steel Moment Frame. *Earthquake Engineering and Structural Dynamics* **40:7**, 807–825.

Suita, K., Yamada, S., Tada, M., Kasai, K., Matsuoka, Y., and Shimada, Y. (2008). Collapse Experiment on 4-Story Steel Moment Frame Part 2: Detail of Collapse Behavior. *14th World Conference on Earthquake Engineering*, Paper No. 14-S17-01-011.

Krishnan, S. and Muto, M. (2012). Mechanism of Collapse of Tall Steel Moment Frame Buildings Under Earthquake Excitation. *Journal of Structural Engineering* **In Print**.

Muto, M. and Krishnan, S. (2011). Hope for the Best, Prepare for the Worst: Response of Tall Steel Moment Frame Buildings to the ShakeOut Scenario Earthquake. *Earthquake Spectra* **27:2**, 375-398.